Silicon based oxidation-resistant coatings on Ti6242 alloy by dynamic ion mixing

J.P. Rivière, L. Pichon, M. Drouet, A. Galdikas and D. Poquillon

Laboratoire de Métallurgie Physique, University of Poitiers, Poitiers, France[b]Kaunas University of Technology, Kaunas, Lithuania
CIRIMAT, Institut National Polytechnique de Toulouse, Toulouse, France

Abstract

The influence of Si_xC_y and Si_xN_y amorphous coatings on the oxidation resistance of a Ti6242 (Ti–6Al–2Sn–4Zr–2Mo) alloy was investigated. They were produced at room temperature by the dynamic ion mixing technique combining physical vapour deposition with simultaneous bombardment with 120 keV Ar^+ ions. Isothermal oxidation tests were carried out at 600 °C in 1 atm flowing synthetic air (80% N_2, 20% O_2) demonstrating a considerable reduction (~two orders of magnitude) of the oxidation rate for at least 100 h. The structural modifications after oxidation were investigated by XPS, XRD, SEM, SIMS. The formation of SiO_2 is detected as the main oxidation product in the coating and the formation of Ti–Si compounds is also observed in the coating/substrate interface region. The crystallisation of Si_xN_y is not detected and for Si_xC_y only some traces of β-SiC could exist. The improvement of oxidation resistance of Ti6242 is discussed in relation with the intrinsic properties of the coatings and with the interface mixing and ion beam densification.

Keywords: Protective coating; Oxidation; Titanium alloy; Silicon nitride; Silicon carbide

1. Introduction

The high strength and resistance to both fatigue and creep make modern titanium alloys attractive materials for the compressor blades of gas turbine aero engines operating at temperatures above 500 °C. However at these temperatures the titanium alloys and particularly those of α/β mixed structure are susceptible of rapid oxidation in air as well as α-case formation [1], [2] and [3] because the migration of oxygen promotes the formation of an oxygen-rich Ti hexagonal solid solution (α-phase) and modifies the α/β mixed phase structure near the surface. These modifications due to the inward diffusion of oxygen and particularly the preferential stabilization of the more brittle alpha-phase considerably reduce the mechanical properties of titanium alloys above 500 °C by the increased tendency of crack formation under stress. The research for improving the oxidation resistance of titanium based alloys by various surface treatments and protective coatings has been very active and is stimulated by the need to improve both the durability and engine performance in aerospace industry [4].

A good reduction in oxidation of pure Ti has been obtained by a thin Si coating bombarded with Ar^+ ions to produce interface mixing with the substrate [5], siliconizing at high temperature appears also a promising technique for improving the oxidation resistance of γ-TiAl [6] and [7], silicon nitride ceramic coatings have been also previously applied successfully for improving oxidation resistance of titanium alloys [8] and [9]. It appears that silicon based ceramic coatings exhibit interesting physicochemical properties for oxidation protection of titanium alloys. However they must fulfil two important requirements: strong adhesion and high density (i.e. low porosity or cracks). This means that the durability and performance of a coating will depend critically not only on its intrinsic properties but also on the deposition technique.

It has been demonstrated that the bombardment of a growing film with either low energy Ar^+ ions (6 keV) [10] and [11], or high energy Ar^+ ions (60–300 keV) [12] and [13], produces beneficial modifications in the film structure and interface with the substrate. The process of Ion Beam Assisted Deposition (IBAD) involves bombardment with a low energy ion beam (3–15 keV) simultaneously with the deposition and enables the formation of dense coatings.

The Dynamic Ion Mixing (DIM) is a variant of IBAD using ion beams of higher energy (100–300 keV) to achieve a more efficient interface mixing. The spatial redistribution and atomic transport at the coating/substrate interface is produced at room temperature over relatively long distances and creates an interface of graded composition improving the adhesion of the coating [13] and [14]. The high energy ion bombardment can also modify the structure of the growing film as a result of the high density of displacements and replacements of atoms in collision cascades. These very specific effects contribute to the formation of dense and adherent ceramic coatings on metallic surfaces which are of special interest for corrosion protection applications.

In the present study we have investigated the influence of SiC and Si_xN_y coatings deposited by DIM on the oxidation resistance of a Ti6242 alloy at 600 °C.

2. Experimental conditions

2.1. Material and surface preparation

The Ti6242 alloy exhibits the α/β mixed phase structure analogous to the more conventional TA6V alloy but it can be considered as a nearly α-alloy. The chemical composition is Ti–6Al–2Sn–4Zr–2Mo, the numbers are in weight percentage and the balance is titanium. The samples used for the oxidation experiments consist in discs 15 mm in diameter and 2 mm in thickness. In order to investigate the influence of the surface roughness we have prepared two series of samples: in a first one (sample A) the samples were mechanically polished up to grit 500 on both sides as well as the lateral surface to a mean roughness $R_a \backsim 0.1$ μm, in a second series (sample B) mechanical polishing was performed up to grit 4000. Then the surfaces were polished up to a “mirror” finish using a 1 μm diamond paste, giving a final roughness $R_a \backsim 0.03$ μm. All the samples were ultrasonically cleaned in acetone and ethanol and finally dried.

2.2. Coating deposition conditions

Si_xC_y and Si_xN_y coatings were deposited at room temperature (RT) by ion beam sputtering using a Kaufman type ion source of 7.5 cm diameter and the samples are mounted on a rotating substrate holder. A water cooled target consisting of a sintered disk either SiC or Si_3N_4 of 10 cm diameter was sputtered under a 45° angle of incidence with 1.2 keV Ar^+ ions. The pressure of the chamber before the deposition was $5 \cdot 10^{-5}$ Pa and was maintained at this

pressure during the deposition procedure. All the external surfaces of the samples, including the lateral ones were uniformly coated. The procedure consisted in depositing firstly the Si_xC_y or Si_xN_y coating on the front disc surface; then the chamber was opened and the samples were turned up to deposit on the second disc side; since there is no shadowing of the lateral disc surfaces they are also coated. A calibrated quartz crystal oscillator was used to monitor the growth rate and the final film thickness. The ion beam mixing was performed with 120 keV Ar^+ ions during all the film deposition for Si_xC_y coatings and only on the first 40 nm of deposit for those of Si_xN_y. The measured final film thicknesses were respectively 0.21 μm for Si_xN_y and 0.25 μm for SiC.

2.3. Oxidation tests and characterization methods

The chemical composition of Si_xC_y and Si_xN_y coatings were determined by Rutherford Backscattering Spectrometry and also by XPS. The modification of the surface composition of the coatings was investigated using X-ray photoelectron spectrometer (XPS, ESCALAB MK II). The samples were introduced in the apparatus low pressure chamber (10^{-8} Pa) 12 h before analysis and we used an Ar focussed beam for cleaning the surface of the samples in order to remove surface contamination due to laboratory air. Experiments were carried out using the Mg K_α X-ray radiation ($h\nu$ = 1253.6 eV) and the following binding energies were selected: Al—2p, Si—2s; C—1s; Ti—2p; O—1s.

Depth profile distributions were also performed by glow discharge optical emission spectroscopy (GDOES) and by SIMS experiments (CAMECA IMS4F6 apparatus using Cs^+ ions). Secondary Ion Mass Spectroscopy (SIMS) was used to characterize the coated samples before and after oxidation; surface sputtering was realized with 10 keV Cs^+ ions and a 30 nA current intensity. Cesium atoms, were chosen in order to produce negative ions from electronegative elements such as $O^{2-}Zr^{2-}$.

High temperature oxidation tests have been conducted in SETARAM TAG24S equipment at 600 °C. This apparatus has the advantage of combining good accuracy with a limitation of buoyancy effects due to a symmetrical furnace in which an inert sample counterbalances these effects. Isothermal oxidation tests have been carried out in 1 atm flowing synthetic air (80% N_2, 20% O_2). Heating and cooling rates were always of 1°/s. Dwell time for all the tests was 100 h. The weight gain was continuously measured as a function of time. In this study,

oxidation kinetics during isothermal tests has been analyzed following the procedure detailed in [15].

Scanning electron microscopy (SEM) was used to observe both the surface and cross sections of the oxidized samples. The structure of the oxidized surface layer was investigated by X-Ray diffraction (XRD) using a Siemens D5005 diffractometer with Cu K_α (λ = 0.15406 nm) wavelength either in the symmetric (θ, 2θ) mode or at glancing incidence with a fixed incident angle of 2° or 8°.

3. Results and discussion

The quantitative chemical composition analysis of the coatings deduced from XPS and RBS indicates that Si_xC_y films have almost the equi-atomic composition ($x / y \sim 0.9$) while for Si_xN_y ones the ratio $x / y \sim 2$. The coatings produced by DIM are very dense and free from columnar structure as shown on the SEM micrograph of a fractured Si_xN_y coating presented in Fig. 1. In the as-deposited state, both types of coatings did not reveal any additional diffraction peak by XRD, except those of the substrate showing the amorphous state of these coatings.

Fig. 1. SEM FEG micrographs of the Si_xN_y fractured coating showing the fully dense amorphous structure.

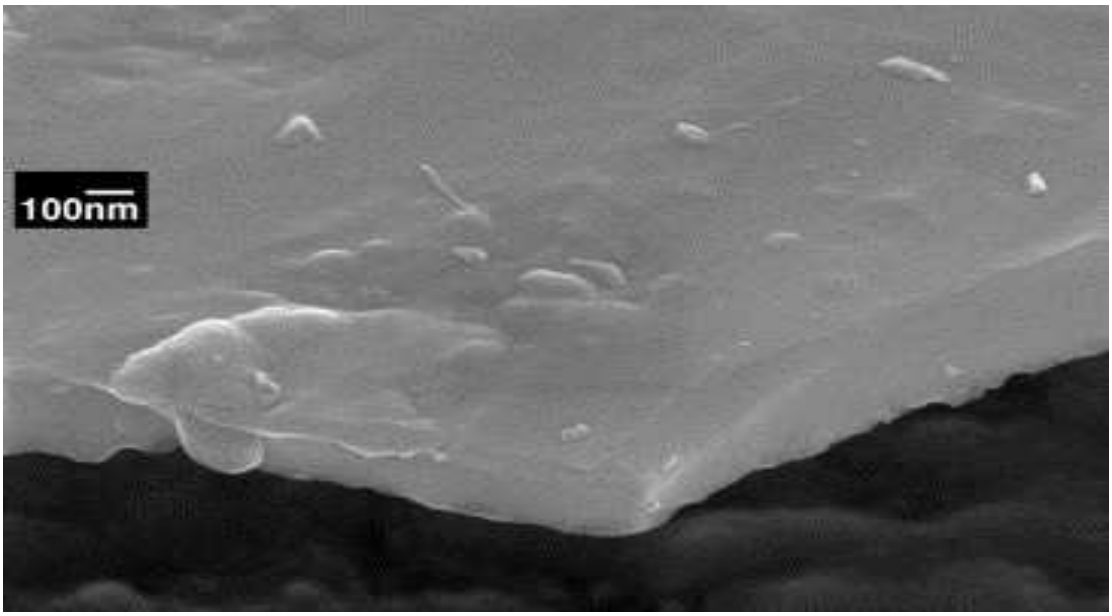

In order to quantify the protective efficiency of the coatings, two uncoated samples have been oxidized in the same conditions: sample A ($R_a \sim 0.1$ μm) and sample B ($R_a \sim 0.03$ μm) (Table

1). Oxidation kinetics at 600 °C are plotted on Fig. 2. The uncoated sample oxidation kinetics follow a parabolic law with oxidation kinetics rates of 4.6 10^{-8} and 4.8 10^{-8} $mg^2\ s^{-1}\ cm^{-4}$, respectively, for sample B and A. These values are in good agreement with the data available in literature for: pure titanium [16] and [17] and Ti–4.02wt.%Al [18]. The surface finishing is known to modify slightly oxidation kinetics explaining why the parabolic rate constant is a little higher for sample A with higher roughness. Table 2 gives the values of the oxidation kinetics rates obtained for the different coated samples. All the coated specimens show very slow oxidation kinetics and the parabolic constant k_p is two orders of magnitude below the values obtained with uncoated samples; we can notice that the coating Si_xN_y-M2 deposited on a mirror polished substrate exhibits the lowest oxidation rate. The comparison between the two different surface preparations (rough finishing or mirror finishing) indicates a slight increase of oxidation kinetics with roughness. SEM observations of the specimen before and after oxidation indicated the localized presence of TiO_2 in some defect of the coating. The silicon base coated samples do not exhibit any degradation except localized attacks in some tiny spot where the coating presents a small crack or pinhole as one can see on SEM micrograph of Fig. 3. When no defect is present, the coating acts as a perfect diffusion barrier and prevents oxidation.

Table 1.

Description of the samples

Substrate Ti6242	**Coating**	**Thickness (μm)**
Sample A ($R_a \sim 0.1$ μm)	Uncoated	
Sample B ($R_a \sim 0.03$ μm)	Uncoated	
Sample A ($R_a \sim 0.03$ μm)	Si_xC_y-M1	0.25
	Si_xN_y-M2	0.21
Sample B ($R_a \sim 0.1$ μm)	Si_xC_y-R4	0.25
	Si_xC_y-R5	0.25
	Si_xN_y-R2	0.21

M1 and M2 are the coatings deposited on mirror polished substrates ($R_a \sim 0.03$ μm) and R4, R5, R2 are the coatings deposited on rough surface ($R_a \sim 0.1$ μm).

Fig. 2. Oxidation kinetics of samples tested at 600 °C in synthetic air. Sample A and sample B are the uncoated Ti6242 substrates with different surface roughness respectively R_a = 0.1 and 0.03 μm; Si_xC_y-M1 and Si_xN_y-M2 are the coatings deposited on mirror polished substrates ($R_a \sim 0.03$ μm) and Si_xC_y-R4, Si_xC_y-R5, Si_xN_y-R2 are the coatings deposited on rough surface ($R_a \sim 0.1$ μm).

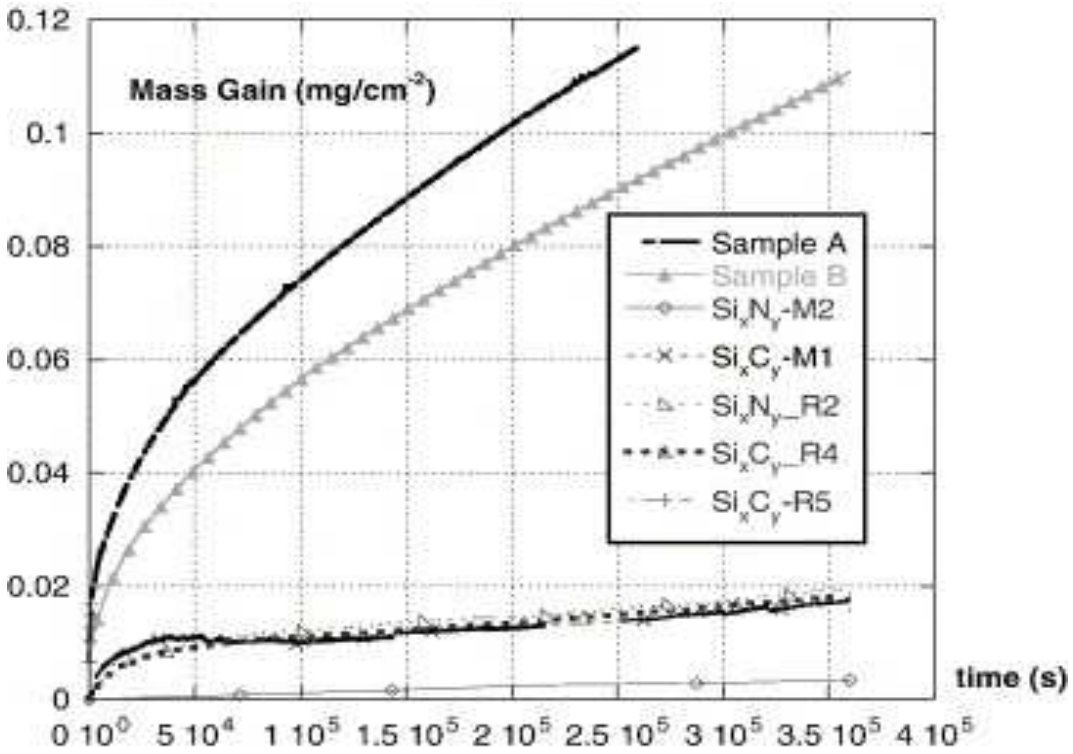

Table 2.

Oxidation kinetics rates under isothermal oxidation (600 °C and synthetic air)

Substrate Ti6242	**Coating**	**k_p ($mg^2\ s^{-1}\ cm^{-4}$)**
Sample A ($R_a \sim 0.1$ μm)	Uncoated	$4.8\ 10^{-8}$
Sample B ($R_a \sim 0.03$ μm)	Uncoated	$4.6\ 10^{-8}$
Sample A ($R_a \sim 0.03$ μm)	Si_xC_y-M1	$7.5\ 10^{-10}$
	Si_xN_y-M2	$1.6\ 10^{-10}$

Substrate Ti6242	Coating	k_p ($mg^2\ s^{-1}\ cm^{-4}$)
Sample B ($R_a \sim 0.1$ μm)	Si_xC_y-R4	$8.4\ 10^{-10}$
	Si_xC_y-R5	$7.2\ 10^{-10}$
	Si_xN_y-R2	$8.0\ 10^{-10}$

Fig. 3. FEG SEM micrograph of a localized pinhole zone showing titanium oxide growth on Si_xN_y coated specimen oxidized 100 h at 600 °C in synthetic air.

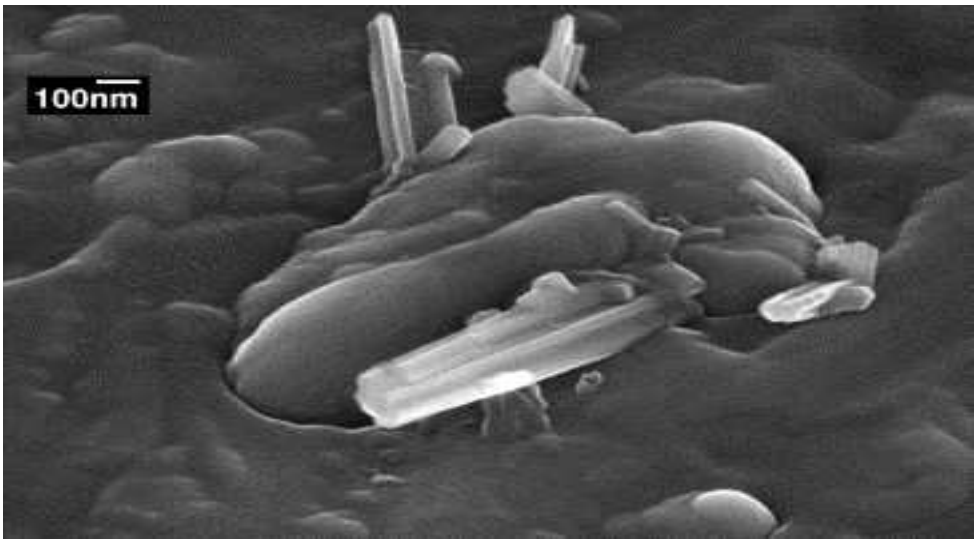

XRD analyses of the uncoated alloy, coated with Si_xC_y before and after oxidation obtained at a grazing angle $\alpha = 2°$ are presented in Fig. 4. We cannot notice any additional peaks when comparing spectra of the uncoated Ti6242 alloy with the Si_xC_y coated one. The only observed peaks belong to the substrate (α-Ti phase dominant), so the coating is XRD amorphous. After oxidation at 600 °C several additional but not well expressed and broad peaks appear. According to JCPDS files the peaks at 26° and 47° belong to SiO_2, the peaks at 45° and 47° are typical for Ti_5Si_4; however the peak at 50° can be explained by the presence of TiSi which is less stable than Ti_5Si_4, no peaks of more stable Ti_5Si_3 compound are observed in the spectra. The broad peaks at 36° and 61° could indicate the presence of β-SiC which would suggest a beginning of crystallisation. So, the main structural evolution after oxidation at 600° consists in the formation of SiO_2 at the surface and TiSi compounds at the interface, eventually some traces of β-SiC could also exist.

Fig. 4. X-ray diffractograms (Cu K_α radiation) at a grazing angle α = 2° of the initial Ti6242 alloy, coated with Si_xC_y film, oxidized Si_xC_y coated alloy (lower curve rough surface, upper curve mirror polished surface).

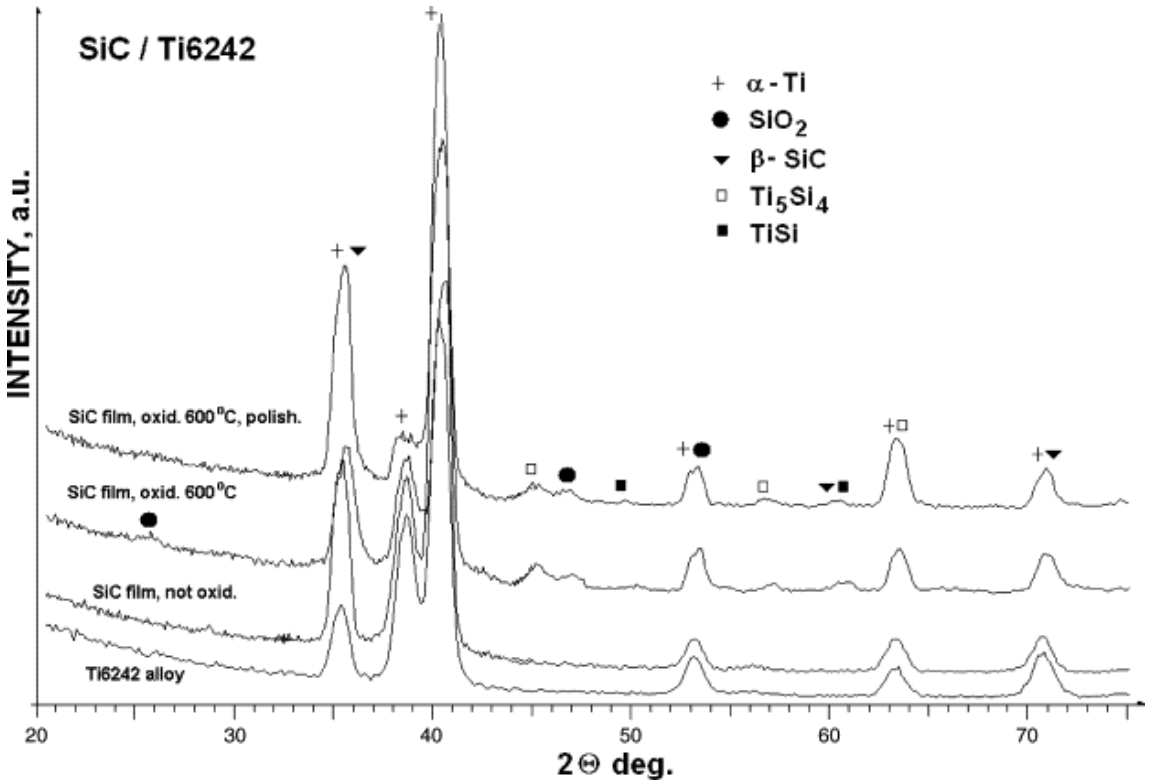

The XRD spectra at grazing angle α = 2° of Si_xN_y films are very similar to spectra of Si_xC_y films as one can see on Fig. 5. One can see that as for previous coatings, the presence of SiO_2 and two types of titanium silicide TiSi and Ti_5Si_4 are observed. An important point to notice is that no crystallisation of Si_xN_y is observed which is in agreement with the high thermal stability of amorphous silicon nitride where the formation of crystallized phase is observed above 1200 °C [19].

Fig. 5. X-ray diffractograms (Cu K_α radiation) at a grazing angle α = 2°: (1) initial Ti6242 substrate; (2) Ti6242 coated with Si_xN_y film, (3) Ti6242 coated with Si_xN_y after oxidation.

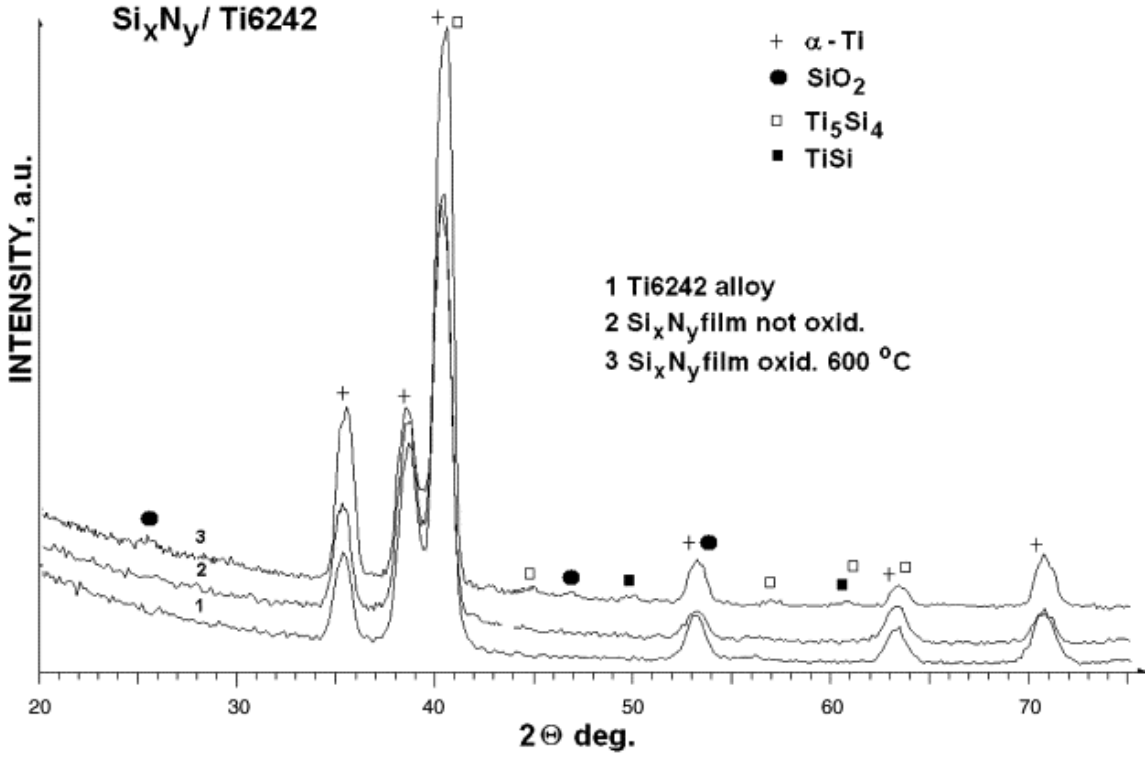

SIMS analysis carried out on non-oxidized and on oxidized Si_xC_y and Si_xN_y samples shows clearly the Zr segregation at the coating/metal interface. We present on Fig. 6 SIMS composition depth profiles of Zr in Si_xN_y coated Ti6242 before and after oxidation at 600 °C; this result is confirmed by GDOES depth profiling. This behaviour was also evidenced on the Ti6242 uncoated samples oxidized in the same conditions. In this case, the segregation occurs at the oxide/metal interface. For both samples Si_xC_y and Si_xN_y, the comparison between the different profiles obtained for an element (Al, CsAl) or (Zr, CsZr) indicates the presence of ZrO_2 and Al_2O_3 oxides at the coating/metal interface.

Fig. 6. SIMS composition depth profiles of Zr in Si_xN_y coated Ti6242 before and after 100 h of oxidation at 600 °C under synthetic air showing Zr segregation at the coating/Ti6242 interface. The Zr depth profiles(Cs^+Zr^{2-}) are compared before and after oxidation.

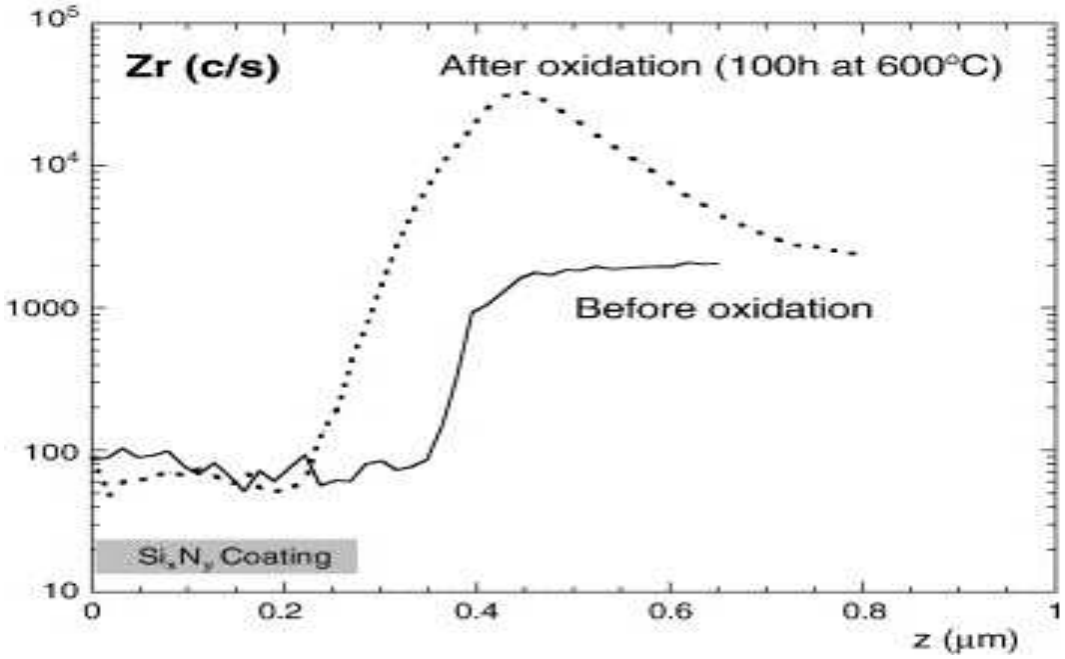

For oxidized Si_xN_y samples, Al, Ti Si and O profiles are not modified by the oxidation. Furthermore, as one can see in Fig. 7 there is no oxygen diffusion into the coating and the Ti6242 substrate since both oxygen profiles before and after oxidation are identical and XPS analyses show that the coating composition remains unchanged.

Fig. 7. SIMS depth profiles of oxygen in Si_xN_y coated Ti6242 showing no oxygen diffusion in the coating after 100 h of oxidation at 600 °C. Oxygen depth profiles ($Cs_2^+O^{2-}$) are compared before and after oxidation.

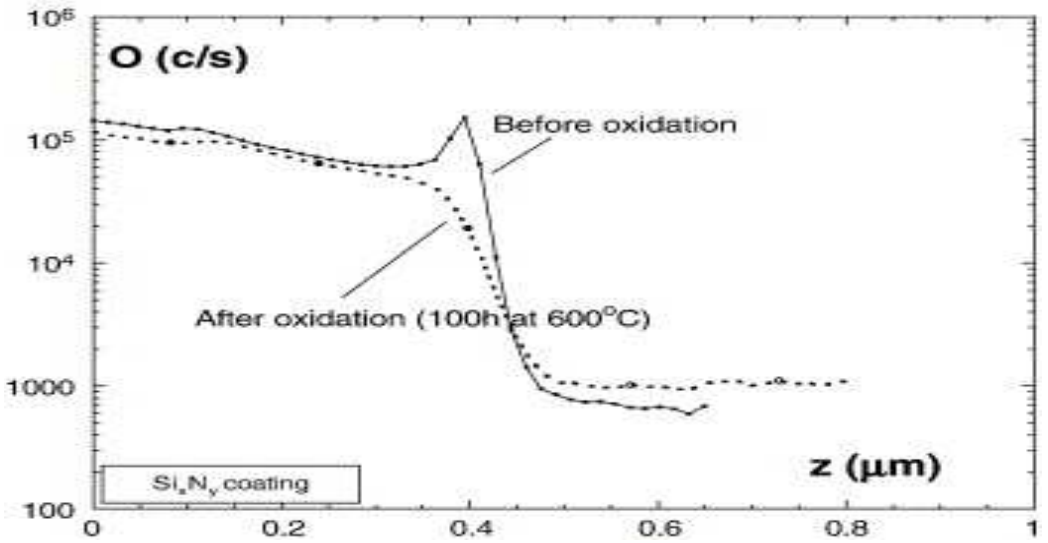

For oxidized Si_xC_y samples, Al, Ti, Si, profiles are not modified by the oxidation treatment but Fig. 8 shows the existence of weak oxygen diffusion into the Ti6242 substrate.

Fig. 8. SIMS depth profiles of oxygen in Si_xC_y coated Ti6242 showing no oxygen diffusion in the coating after 100 h of oxidation at 600 °C. Oxygen depth profiles ($Cs_2^+O^{2-}$) are compared before and after oxidation.

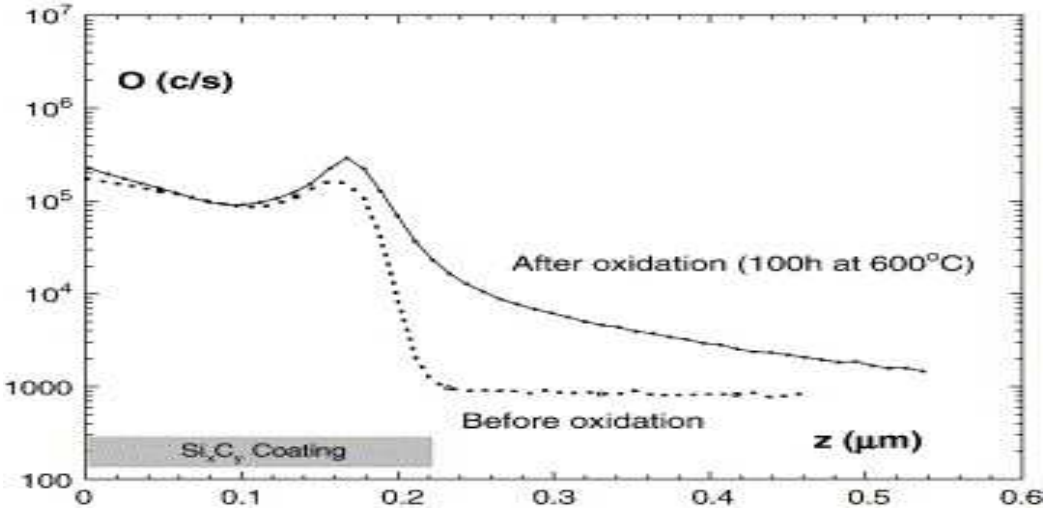

There are several reasons for the excellent oxidation protective effect of Si_xC_y and Si_xN_y amorphous coatings deposited on Ti6242 substrates. The first one is related with the intrinsic physicochemical properties of amorphous Si based coatings which are known to be very good candidates for oxidation and corrosion protection [20], [21] and [22] as long as the temperature is well below their crystallisation temperature. For this reason Si_xN_y is certainly a better choice since crystallisation occurs at higher temperatures and solid state reaction with Ti occurs only above 850 °C [23], for amorphous SiC coatings the very beginning of crystallisation becomes detectable by HRTEM at 750 °C [24]. Both Si_xC_y and Si_xN_y coatings do not exhibit stoichiometric compositions, and it is suggested that high Si contents in the coatings may promote the formation of a thin surface layer rich in SiO_2 acting as a diffusion barrier for oxygen. The second reason of improved oxidation protection comes from the specific advantages of the DIM technique itself producing an intermixed layer giving rise to a gradual transition from substrate to layer which spreads stresses over a longer distance compared with sharp short-range transitions characterizing most of deposition techniques, and reduces their intensity. In addition, energy and momentum transfer from incident ions to condensing atoms lead to rearrangement of the surface structure by enhanced surface and bulk diffusion, so closure of voids and micropores takes place producing dense coatings. The above results obtained for rough surfaces indicate also the high degree of general coverage obtained by the DIM technique.

4. Conclusions

High precision thermogravimetry measurements during isothermal oxidation at 600 °C has shown that thin SiC and Si_xN_y coatings deposited by dynamic ion mixing are able to provide an efficient protection against oxidation of Ti6242 alloy at 600 °C for at least 100 h. Coatings have been tested on substrates with two different surface roughnesses and the protective effect of coatings remains efficient with a rough surface preparation. The DIM technique appears to be appropriate for producing dense coatings with high adhesion and very low microporosity suited for long-term oxidation protection. Cyclic oxidation at 600 °C will be carried out in order to confirm these results.

Acknowledgements

This work is supported by the Ministère de la Recherche in the framework of RNMP network contract APROSUTIS; the participants are academic laboratories: LMP and LMPM (Poitiers), CEMES-CNRS and CIRIMAT (Toulouse), LGP (ENIT Tarbes), and laboratories from industries: SNECMA Moteurs (DMA Corbeil and DMS Vernon), AIRBUS France (Toulouse) and TURBOMECA (Bordes). The Ti6242 samples were kindly provided by TURBOMECA company. A. Galdikas thanks region Poitou-Charentes for financial support. The authors gratefully thank M. Gérard Chatainier for XPS analysis and M. Claude Armand for SIMS analysis.

References

I. Gurappa, *Mater. Sci. Eng., A Struct. Mater.: Prop. Microstruct. Process.* 356 (2003) (1/2), p. 372.

W.J. Boettinger, M.E. Williams, S.R. Coriell, U.R. Kattner and B.A. Mueller, *Metal. Mater. Trans. B* 31B (2000) (6), p. 1419.

M.N. Mungole, N. Singh and G.N. Mathur, *Mater. Sci. Technol.* 18 (2002) (1), p. 111.

W. Kaysser, *Surf. Eng.* 17 (2001) (4), p. 305.

A. Galerie, M. Caillet, M. Pons and G. Dearneley, *Nucl. Instrum. Methods* B19/20 (1987), p. 708.

X.Y. Li, S. Taniguchi, Y. Matsunaga, K. Nakagawa and K. Fujita, *Intermetallics* 11 (2003) (2), p. 143.

W. Liang and X.G. Zhao, *Scr. Mater.* 44 (2001), p. 1049.

C.J. Bedell, H.E. Bischop, G. Dearneley, J.E. Desport, H. Romary and J.M. Romary, *Nucl. Instrum. Methods Phys. Res. Section B* 59/60 (1991) (1), p. 245. X. Dong, Z. Zhihong, L. Xianghuai and Z. Shichang, *Surf. Coat. Technol.* 66 (1994) (1–3), p. 486.

G. Dearnaley, *Nucl. Instrum. Methods* 182–183 (1981) (2), p. 899.

W. Ensinger and G.K. Wolf, *Mater. Sci. Eng.* A116 (1989), p. 1.

J. Von Stebut, J.P. Riviere, J. Delafond and C. Sarrazin, *Mater. Sci. Eng.* A115 (1989), p. 267.

J.P. Riviere, *Surf. Coat. Technol.* 108–109 (1998) (1–3), p. 276

M. Kiuchi, *Nucl. Instrum. Methods Phys. Res.* B80/810 (1993), p. 1343.

D. Monceau and B. Pieraggi, *Oxid. Met.* 50 (1998) (5/6), p. 477.

P. Kofstad, K. Hauffe and H. Kjollesdal, *Acta Chem. Scand.* 12 (1958), p. 259.

P. Kofstad, High Temperature Oxidation of Metals, Wiley, NY (1966).

A.M. Chaze and C. Coddet, *J. Less-Common Met.* 157 (1990), p. 55.

H. Schmidt, W. Gruber, G. Borchardt, M. Bruns, M. Rudolphi and H. Baumann, *Thin Solid Films* 450 (2004) (2), p. 346.

K. Baba, R. Hatada, R. Emmerich, B. Enders and G.K. Wolf, *Nucl. Instrum. Methods Phys. Res. Section B* 106 (1995) (1–4), p. 106.

F. Sibieude, J. Rodriguez and M.T. Clavaguera-Mora, *Thin Solid Films* 204 (1991) (1), p. 217.

X. Liu, Y. Yu, Z. Zheng, W. Huang, S. Zough, Z. Jin, M. Chang, S. Xu, S. Taniguchi, T. Shibata and K. Nakamura, *Surf. Coat. Technol.* 46 (1991) (2), p. 227.

R.E. Loehman, A.P. Tomsia, J.A. Pask and S.M. Johnson, *J. Am. Ceram. Soc.* 73 (1990), p. 552.

H. Mori and T. Sakata, *Nucl. Instrum. Methods Phys. Res.* B94 (1994), p. 73.

Original text : Elsevier.com